Supporting Information for:

In Situ Transmission Electron Microscopy Study of Electron Beam-Induced Transformations in Colloidal Cesium Lead Halide Perovskite Nanocrystals

Zhiya Dang,[1] Javad Shamsi,[1,2] Francisco Palazon,[1] Muhammad Imran,[1,2] Quinten A. Akkerman,[1,2] Sungwook Park,[1,3] Giovanni Bertoni,[1,4] Mirko Prato,[1] Rosaria Brescia,[1,] and Liberato Manna[1,*]*

[1]Department of Nanochemistry, Istituto Italiano di Tecnologia, Via Morego 30, 16163 Genova, Italy

[2]Dipartimento di Chimica e Chimica Industriale, Università degli Studi di Genova, Via Dodecaneso, 31, 16146, Genova, Italy

[3]Department of Physics, Pukyong National University, Busan 608-737, Korea

[4]IMEM-CNR, Parco Area delle Scienze 37/A, Parma, 43124, Italy

1. EDS analysis of the evolution of $CsPbBr_3$ nanosheet composition upon electron beam irradiation

EDS analyses were carried out for 3 nm thick nanosheets under electron irradiation at incident electron energy (E_0) of 80 keV and 200 keV (Figure S1(a)). After exposure to a comparable electron dose, the Br atomic concentration (at.%) varies from 55% to 40% for E_0 = 80 keV and from 57% to 52% for E_0 = 200 keV, which demonstrates a more substantial compositional change at lower E_0. This result proves that a radiolysis mechanism rather than knock-on damage is dominating the loss of Br. Figure S1(b, c) shows Br desorption at low temperatures.

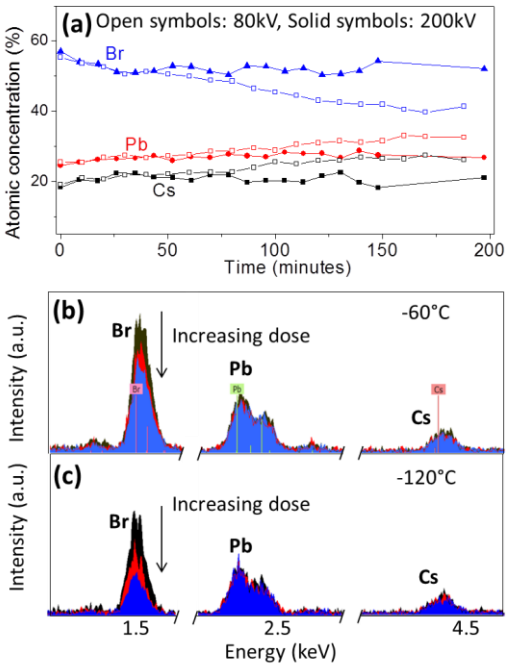

Figure S1. (a) Atomic concentration (at.%) of Cs, Pb, Br for 3 nm thick $CsPbBr_3$ nanosheets versus electron irradiation time from quantitative EDS measurements at RT for both E_0 = 80 keV (open symbols) and 200 keV (solid symbols); (b) EDS spectra in the energy range of interest for $CsPbBr_3$ nanosheets after being irradiated with 200 keV electrons at three different doses at -60 ºC; (c) same as (b), but at -120 ºC.

Desorption of Br is obviously demonstrated by the STEM-EDS elemental maps in Figure S2 (E_0 = 80 keV). The yellow boxed-region (Figure S2(a)) has been irradiated for an extra duration of around

90 minutes than the surrounding regions before acquisition, and the mapping area (green boxed-region) comprises two areas exposed to different doses: the left, higher dose and the right, lower dose, for which the HAADF-STEM image is shown in Figure 2(b). A significantly lower signal of Br is evident in the elemental maps of left area (higher dose) (Figure S2(c)).

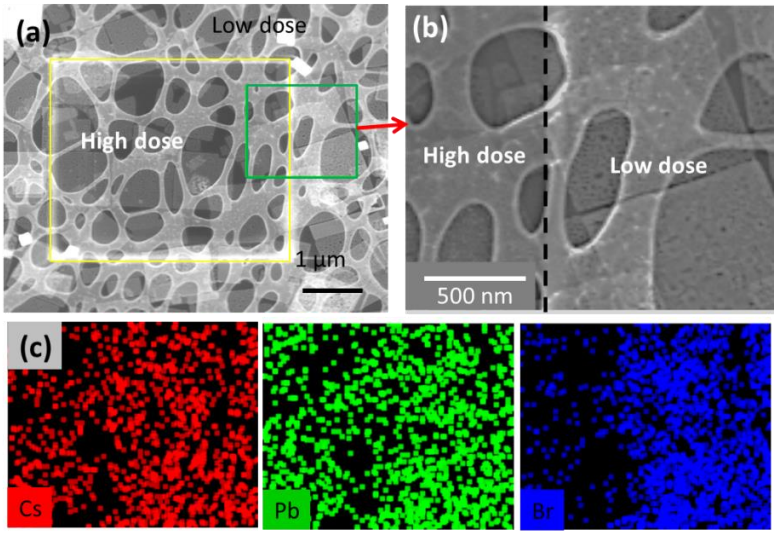

Figure S2. (a) HAADF-STEM image of a group of well-spread 3 nm thick $CsPbBr_3$ nanosheets, among which the sheets in the central yellow boxed-region were irradiated for longer duration (extra 97 minutes) than the surrounding regions before acquisition of EDS maps (E_0 = 80 keV); (b) Magnified view of the area for acquisition of EDS maps: the green-boxed region in (a), which is at the boundary regions between areas exposed to different electron doses; (c) EDS elemental maps for Cs, Pb, Br for region in (b).

2. Pb nanoparticle formation in $CsPbI_3$, $CsPbCl_3$, and Cs_4PbBr_6 nanocrystals and desorption of halogen atoms

High contrast particles have also been observed in $CsPbI_3$ nanowires (Figure S3(a-b)) and $CsPbCl_3$ nanocuboids (Figure S3(d-e)) under electron irradiation. These nanoparticles formed upon irradiation are made of metallic Pb, as supported by crystal structure analyses of Figure S3(c) and Figure S3(f), respectively. Moreover, desorption of Cl with increasing electron dose has been observed during EDS measurement as well (Figure S3(g)). Similar processes (nucleation of Pb

nanoparticles and electron stimulated desorption of Br) have been observed also on Cs_4PbBr_6 NCs, as reported in Figure S3(h, i).

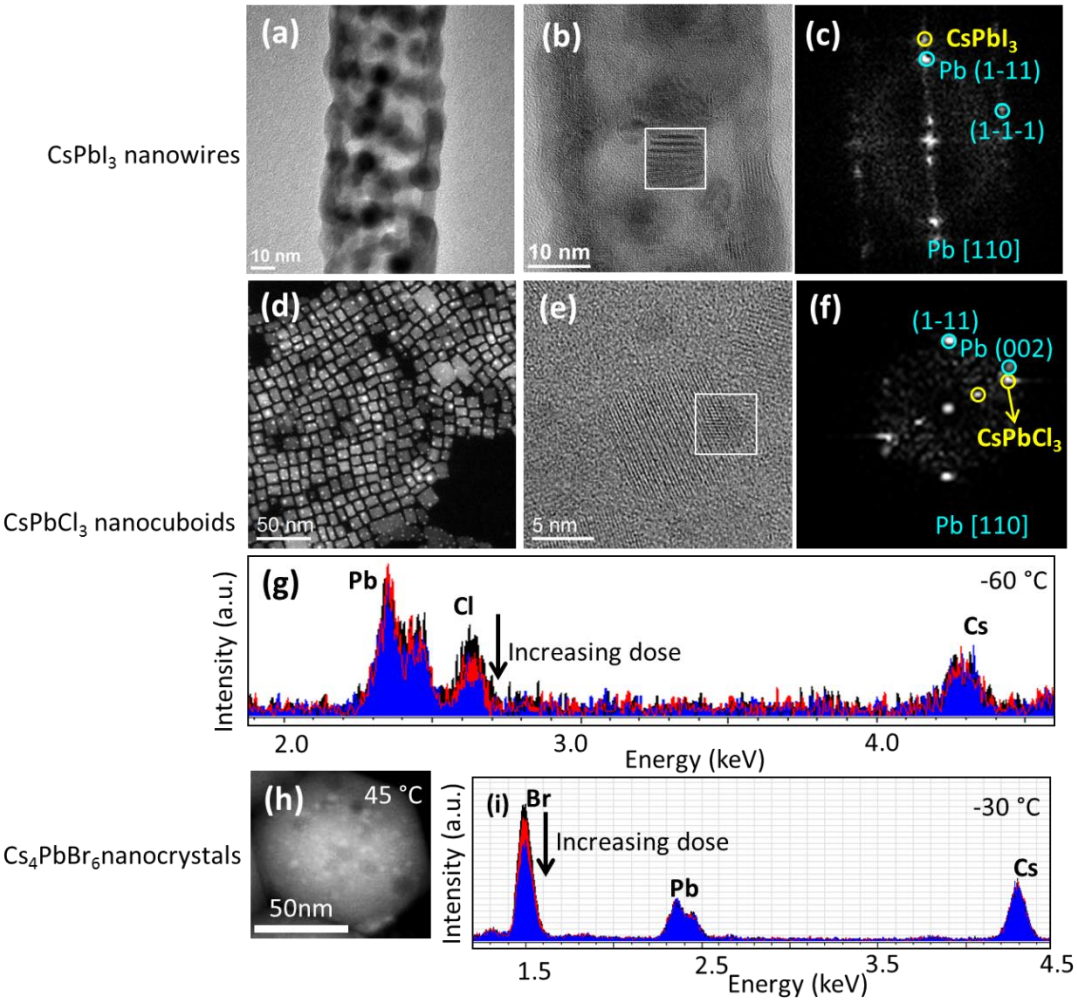

Figure S3. Effect of electron irradiation on $CsPbX_3$ NCs of other halides (Cl and I) and on Cs_4PbBr_6 NCs (E_0 = 200 keV). (a-c) Overview TEM, HRTEM images and corresponding FFT of white boxed-region showing Pb nanoparticle formed on $CsPbI_3$ nanowires (RT); (d) HAADF-STEM and (e-f) HRTEM images and corresponding FFT of white boxed-region showing Pb nanoparticle formed on $CsPbCl_3$ nanocuboids (RT); (g) EDS spectra showing electron stimulated Cl desorption from $CsPbCl_3$ nanocuboids (-60 °C); (h) HAADF-STEM image of Pb nanoparticles formed on Cs_4PbBr_6 NCs (45 °C) and (i) EDS spectra showing electron stimulated Br desorption from Cs_4PbBr_6 NCs (-30 °C).

3. Pb^{2+} reduction and Br desorption under X-ray irradiation

Exposure to other types of irradiation, such as X-rays (1486.6 eV) from the XPS spectrometer, over long exposure times (*i.e.*, 12 hours), was also found to induce Pb^{2+} reduction in the $CsPbBr_3$ nanosheets, Figure S4(a). The amount of Pb^0 increases slightly with longer X-ray exposure time (Figure S4(b)). Figure S4(c) shows the atomic concentration (at.%) of the three elements with irradiation time. The linear fits of the data points are the following: y = -0.084x + 69 for Br; y = 0.04x + 18.2 for Pb, and y = 0.04x + 12.7 for Cs. The negative slope for Br suggests a slight Br desorption under X-ray exposure, with the corresponding increase of the relative concentrations (at.%) of Cs and Pb as shown by their positive slopes. Note that only an average information over thinner and thicker nanosheets is attained by XPS, as opposed to STEM-EDS results which allow instead to discriminate between the two types of NCs (see Figure S7).

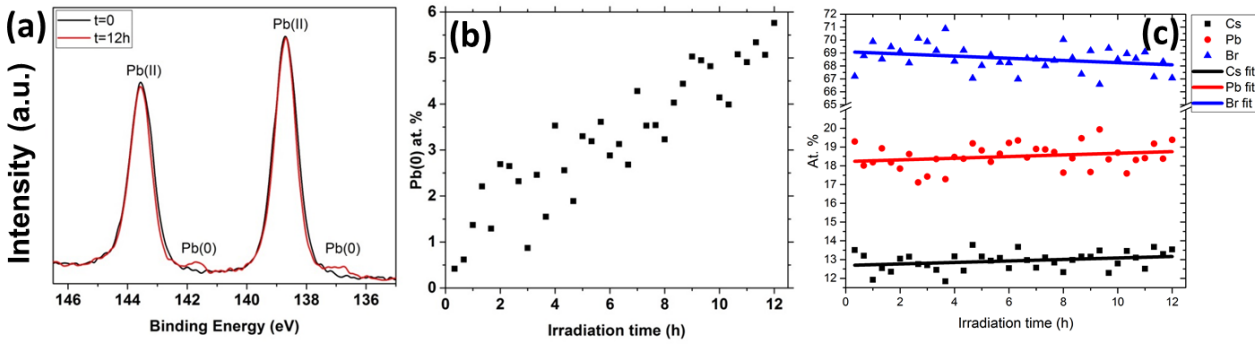

Figure S4. Effect of X ray irradiation on $CsPbBr_3$ nanosheets (1486.6 eV, flux: 2.4 x 10^{11} photons/mm^2/s): (a) XPS spectra taken before and after exposure to X-rays showing two Pb 4f doublets assigned to Pb(II) (Pb(II) $4f_{7/2}$ at binding energy 138.7 eV) and Pb(0) (Pb(0) $4f_{7/2}$ at binding energy 136.9 eV); (b) Evolution of atomic concentration (at.%) of Pb^0 relative to total Pb (Pb(0)/Pb(II)+Pb(0)) versus X-ray exposure time; (c) Atomic concentration (at.%) of Cs, Pb, Br with respect to X-ray exposure time, with respective linear fits showing slow desorption of Br (averaged over thin and thick nanosheets in the entire sampling area).

4. Effect of temperature

HRTEM images acquired for 3 nm thick $CsPbBr_3$ nanosheets at -20 °C and -60 °C are shown in Figure S5(a) and (b) respectively, showing no visible Pb nanoparticles at -60 °C, while small Pb nanoparticles have formed at -20 °C.

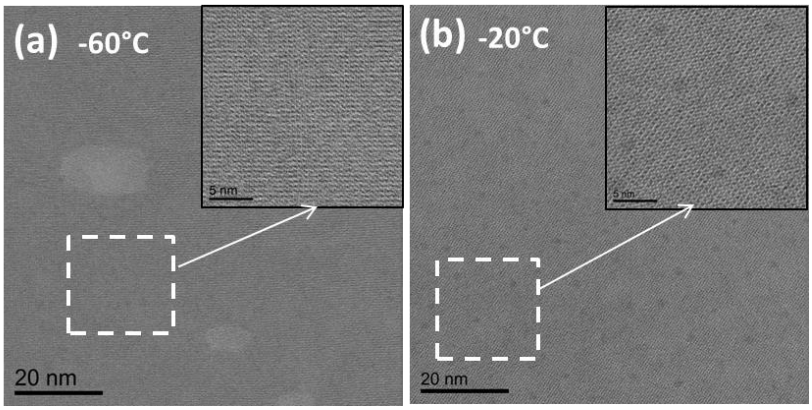

Figure S5. HRTEM images of 3 nm thick $CsPbBr_3$ nanosheets acquired at E_0 = 200 keV at two temperatures: (a) -60 °C (dose: 480 $e^-/Å^2$); (b) -20 °C (dose: 1480 $e^-/Å^2$). Insets are magnified views of the white-boxed regions.

5. Electron beam heating

The temperature change (ΔT) induced by the beam is usually negligible in the TEM.[1] For instance, a 5 nA probe incident on a carbon film with thermal conductivity of 1.6 W/m/K induces a ΔT between 0.5 to 1.4 K at E_0 = 200 keV, depending on beam diameter (from 1 nm to 1 μm). Regarding the present case, Figure S6 reports HAADF-STEM images documenting the formation of the Pb nanoparticles under 200 keV electron irradiation, with different dose rates, at RT and -20 °C. At lower range of dose rate (from 10^5 to 10^8 $e^-/Å^2/s$), the size of the Pb nanoparticles is hardly affected, indicating negligible electron beam heating. When the dose rate increases to about 10^9 $e^-/Å^2/s$, larger Pb nanoparticles are produced. The dose rate used is about 10^7 $e^-/Å^2/s$ for STEM acquisition throughout this work, and the dose rate for HRTEM is also well below the high dose rate range. Therefore, electron beam heating does not play a relevant role on our samples at E_0 =

200 keV.[1, 2] We obtain ΔT (80 keV) = 1.6 ΔT (200 keV) from a brief deduction, which can still be considered negligible.

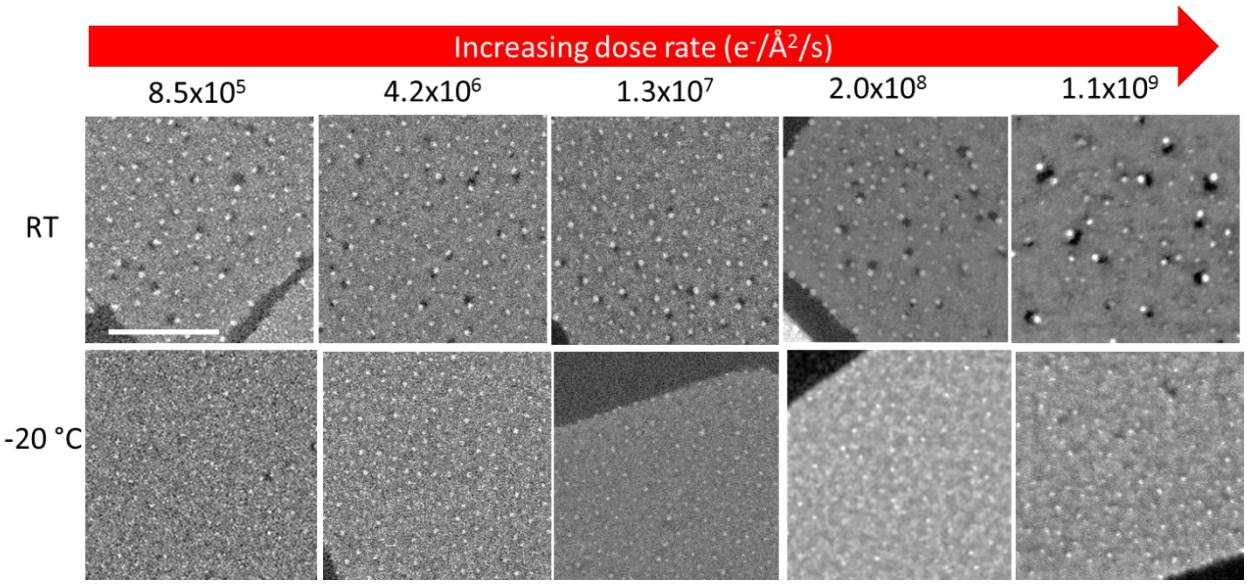

Figure S6. Effect of dose rate on the size of Pb nanoparticles at RT and at -20 °C (Scale bar: 50 nm, E_0 = 200 keV).

6. Formation of Pb nanoparticles in $CsPbBr_3$ NCs with different surface-to-volume ratios

Figure S7(a) plots the change in atomic concentrations (at.%) for 3 nm thick nanosheets and a thicker nanosheet (> 10 nm thick) under 200 keV electron irradiation, which is a clear indication of the pivotal role of surface in degradation of these materials under the electron irradiation. Figure S7(b, c) shows the HAADF-STEM images of $CsPbBr_3$ nanosheets with both thicknesses under similar electron irradiation conditions at RT. On 3 nm thick nanosheets electron irradiation creates voids and the majority of Pb nanoparticles are distributed at the edge of the voids (Figure S7(b)). Pb nanoparticles form only on the surface of thick $CsPbBr_3$ nanosheets under 200 keV electron irradiation (Figure S7(c)).

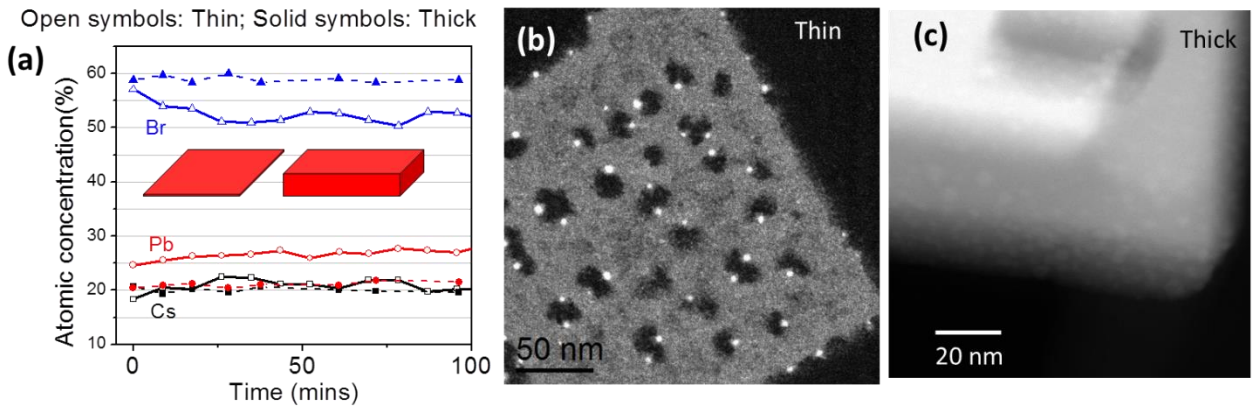

Figure S7. $CsPbBr_3$ nanosheets with different thicknesses (E_0 = 200 keV, RT): (a) Atomic concentration (at.%) of 3 nm thick nanosheets (open symbols) and thicker nanosheet (> 10 nm thick, solid symbols) versus electron irradiation time from quantitative EDS measurements; (b, c) HAADF-STEM images of (b) 3 nm thick nanosheet; (c) > 10 nm thick nanosheet.

Additionally, the comparison between quantitative EDS data collected on thin (3 nm thick) and thick (> 10 nm thick, a minor fraction of them) nanosheets in the analyzed sample provides useful indications on the surface termination of these 2D NCs. At the beginning of our STEM-EDS experiments (Figure S7(a)), the thicker nanosheets exhibit stoichiometric composition (atomic ratio Cs:Pb:Br = 1.0:1.0:3.0), while the thin nanosheets are slightly Cs-deficient (Cs:Pb ≈0.8:1). The latter value may suggest a $PbBr_6$ surface termination.

The nanocuboids with edge length of 8 nm decompose from the corners (Figure S8) by forming Pb nanoparticles at the corners. Following the image in Figure S8(a), two more images from the same area were acquired after increasing the irradiation time (not shown here). Figure S8(b) shows the reduction in size of $CsPbBr_3$ nanocuboids 1-3 in (a) as a function of the irradiation time.

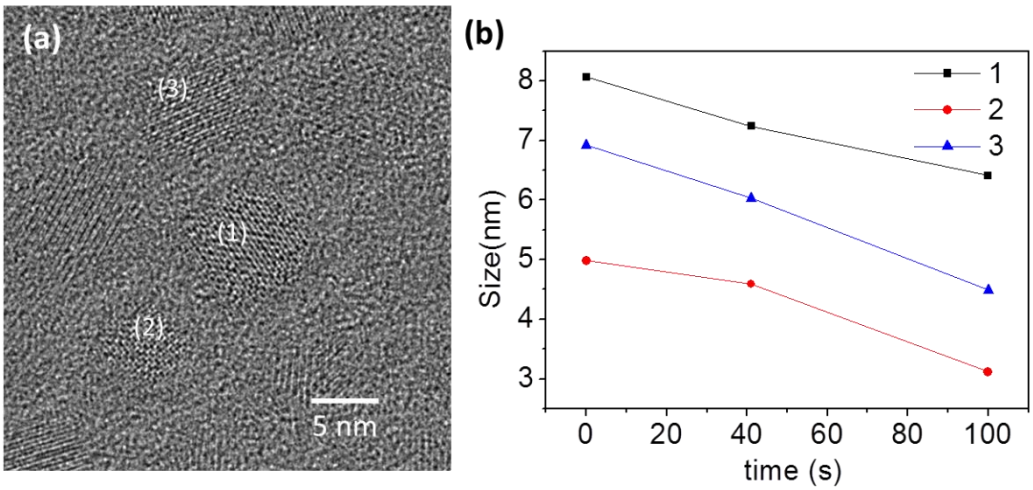

Figure S8. Decomposition of $CsPbBr_3$ nanocuboids (edge length 8 nm) upon 200 keV electron irradiation at RT: (a) HRTEM image of several nanocuboids at time $t=t_0$; (b) Lateral size (diameter) of the cuboids labelled in (a), with respect to the time of electron irradiation.

As discussed, in the 3 nm thick nanosheet voids accompanied with Pb nanoparticles are observed, Figure S7(b). On thicker nanosheets, Pb nanoparticles form on the surface, while the inner $CsPbBr_3$ crystal structure remains, Figure S7(c). Similarly, these processes do not cause the large nanocuboids (edge length of 20~40 nm) to decompose or the nanowires (20 nm wide) to break (Figure 4). However, increasing the temperature not only increases the diffusion of Pb^0 atoms and of clusters of atoms along the surface, but it also enables the diffusion from the inner perovskite lattice, thus enhancing the formation of large Pb nanoparticles and causing significant damage even to these large NCs (Figure S9).

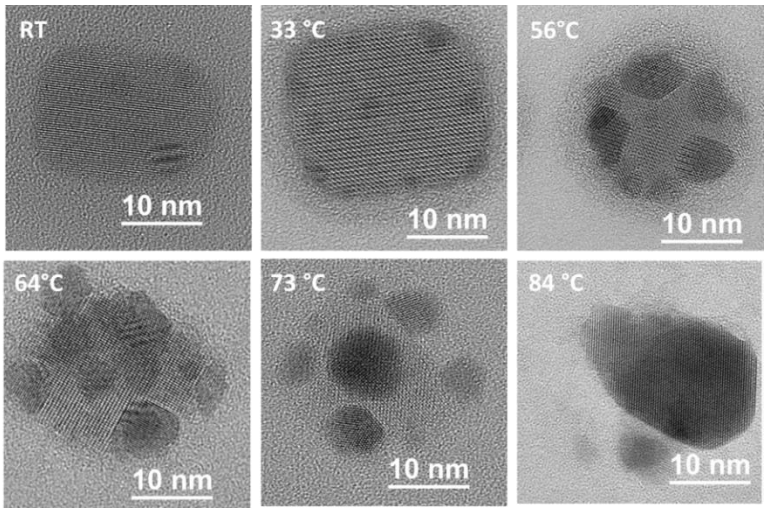

Figure S9. Enhanced Pb nanoparticles formation process with increasing temperature in more bulk-like $CsPbBr_3$ NCs (nanocuboids with edge length of 20~40 nm) (E_0 = 200 keV).

7. Instability of Pb nanoparticles with electron irradiation

In analogy to Pb nanoparticles formed at RT, Pb nanoparticles formed at -40 °C (Figure S10(a, b)) also "disappear" with further electron irradiation (Figure S10(c, d)).

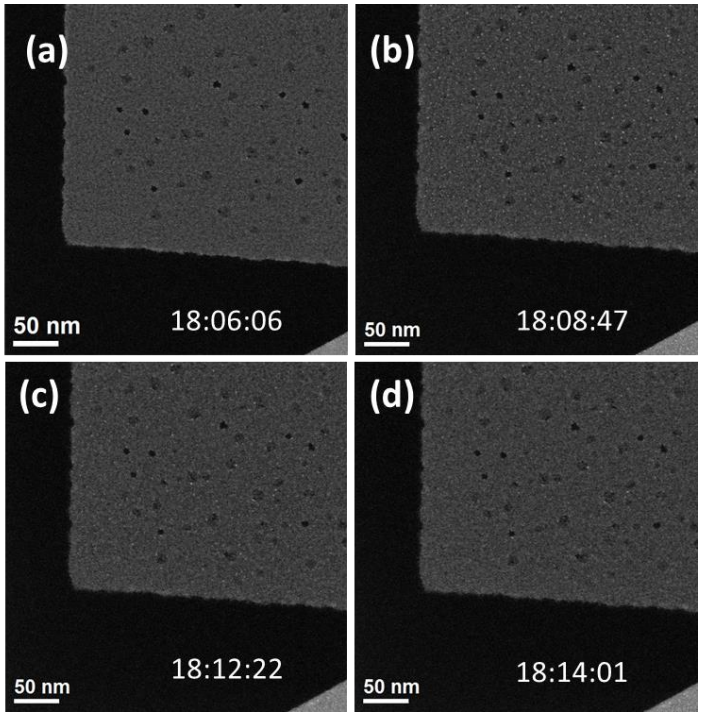

Figure S10. Evolution of Pb nanoparticles in a 3 nm thick $CsPbBr_3$ nanosheet at -40 °C (E_0 = 200 keV).

The “disappearance” of Pb nanoparticles is evident from elemental maps acquired for two voids on a 3 nm thick $CsPbBr_3$ nanosheet in Figure S11. The void shown in Figure S11(a) has formed after irradiation with a lower electron dose, for which Pb nanoparticles distribute at the edge of the void. In comparison, Figure S11(b) shows a void that has been irradiated with a higher electron dose, in which case the Pb nanoparticles form first and then disappear with further electron irradiation.

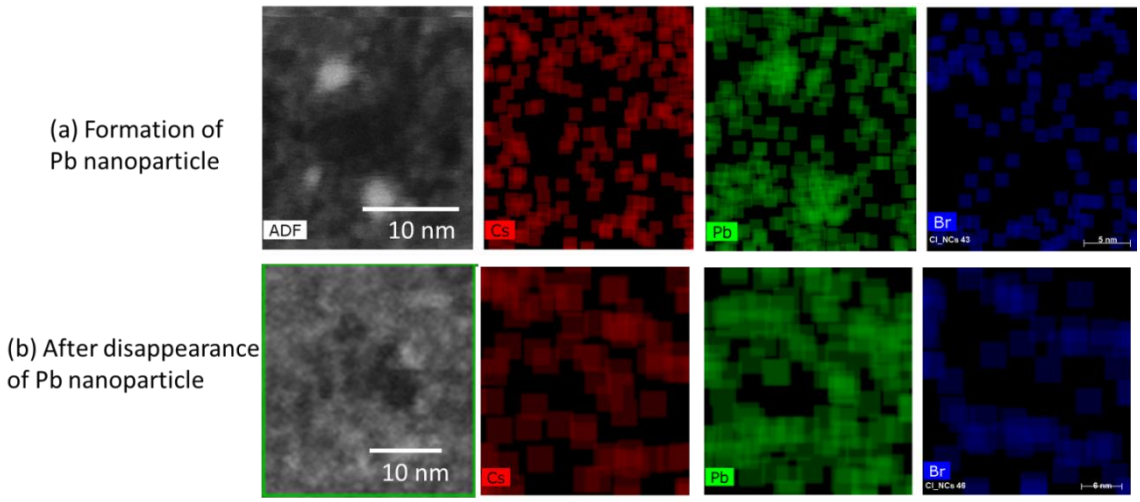

Figure S11. STEM-EDS elemental maps of two voids on a 3 nm thick $CsPbBr_3$ nanosheet: (a) a void accompanied with Pb nanoparticles at a lower dose; (b) a void region after disappearance of Pb nanoparticles at a higher dose (E_0 = 200 keV).

Additional details on the “disappearance” of Pb nanoparticles are revealed by HRTEM observations and reported in Figure S12 and Figure S13. The Pb nanoparticles first amorphize and then dismantle with further electron irradiation. The disappearance of Pb nanoparticles is a dissipation process involving diffusion and spreading out of atoms under electron irradiation.

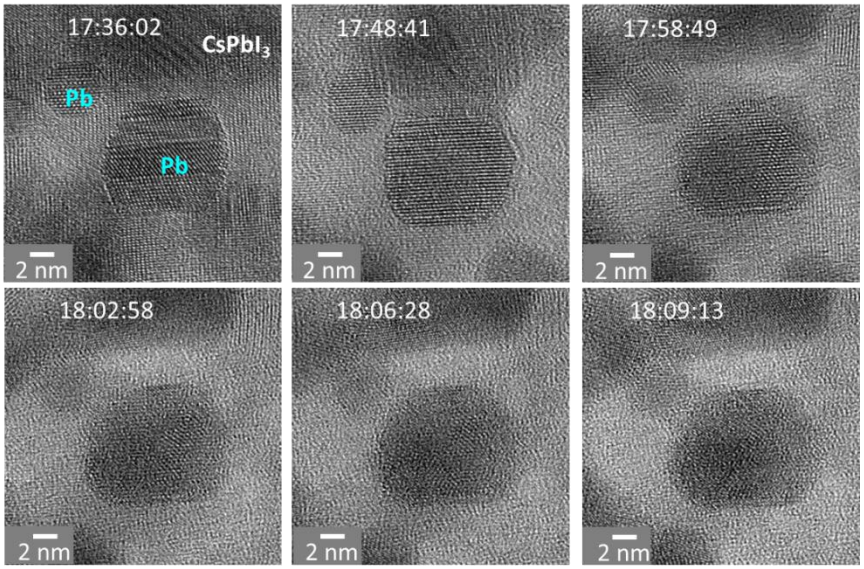

Figure S12. Evolution of Pb nanoparticles with electron irradiation on a 100 nm $CsPbI_3$ nanowire (E_0 = 200 keV, RT).

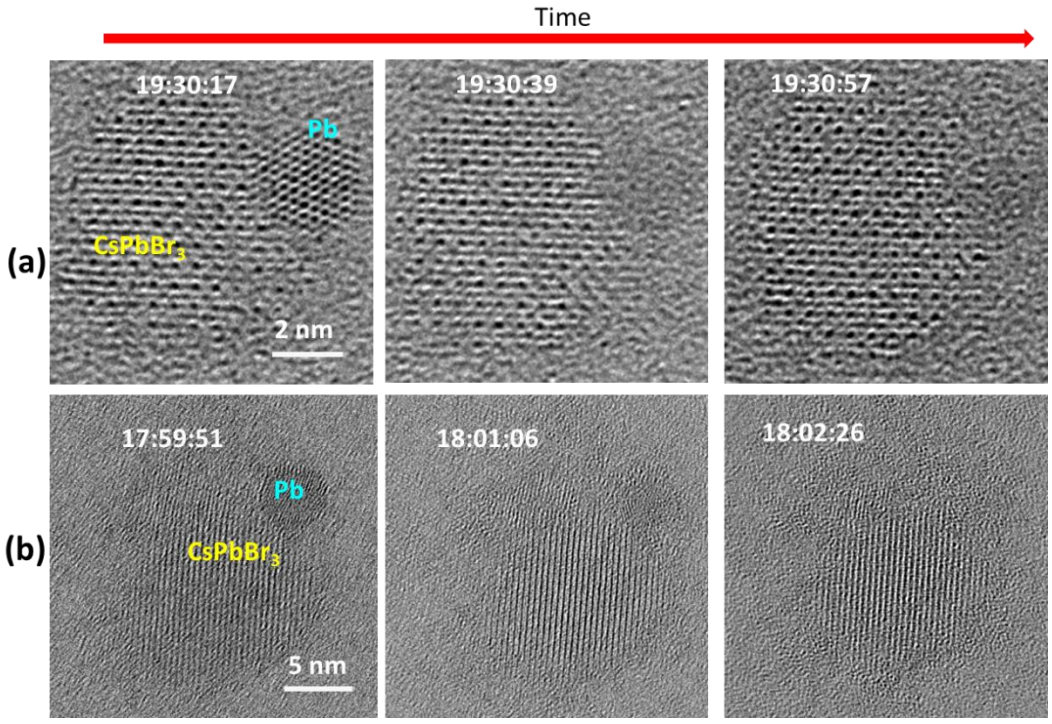

Figure S13. Time evolution of Pb nanoparticles under electron irradiation (E_0 = 200 keV, RT) on (a, b) a $CsPbBr_3$ nanocuboid (edge length 8 nm).

For arrays of $CsPbBr_3$ nanocuboids, this diffusion and spreading out of atoms under continuous irradiation lead to hollow frames, following the initial contours of arrays, Figure S14.

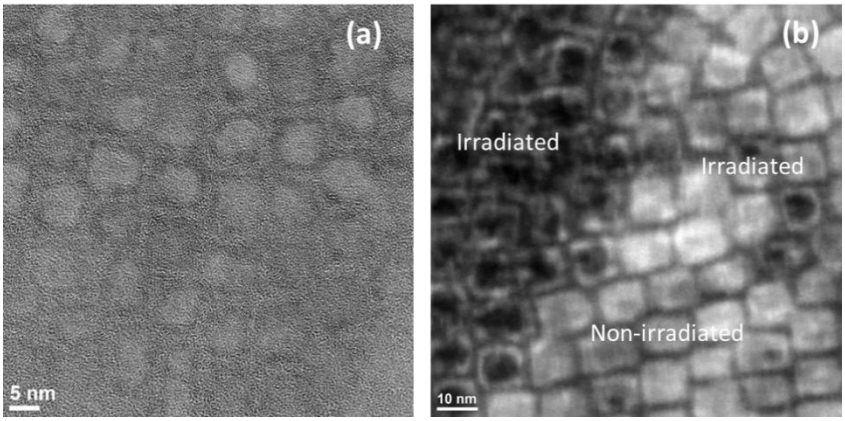

Figure S14. Diffusion of atoms into empty space on the substrate after long electron irradiation (E_0 = 80 keV, RT) on $CsPbBr_3$ nanocuboid arrays (edge length 8 nm): (a) HRTEM; (b) HAADF-STEM.

As shown in Figure S15, under continuous electron irradiation the diffusion of Pb atoms causes firstly the disappearance of the smaller Pb particles, followed by the disappearance of the larger ones. At some locations, two or more Pb particles are close to each other, and the diffusion of Pb atoms from these adjacent Pb nanoparticles can lead to the formation of new Pb clusters, as labelled by the red circles in Figure S15.

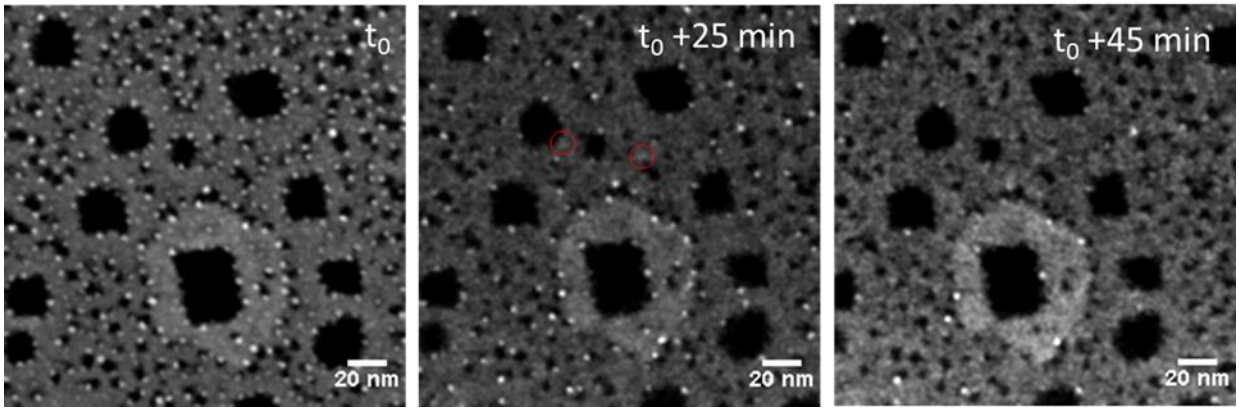

Figure S15. HAADF-STEM images showing dissolution of Pb nanoparticles on 3 nm thick nanosheet via diffusion of atoms. The Pb atoms that diffuse away from the adjacent Pb particles gather and appear as new clusters, some of which are labelled by red circles (E_0 = 200 keV, RT).

8. Syntheses of $CsPbX_3$ (X=Cl, I) and Cs_4PbBr_6 nanocrystals

During the synthesis of $CsPbBr_3$ nanocuboids with edge length of 20~40 nm, in some of the batches, Cs_4PbBr_6 NCs emerged as by-products.

The $CsPbCl_3$ nanocuboids were synthesized with the following procedure: a total amount of 0.188 mmol of $PbCl_2$ and $MnCl_2$ mixture, 5ml ODE (octadecene), 0.5 ml OA (oleic acid), 0.5 ml OLAM (oleyamine) were loaded into a 25 ml two-neck flask and dried at 120 °C for 1h under a vacuum condition. After complete solubilization of chloride salts, the temperature was increased to 180 °C in N_2 atmosphere and 0.4 ml Cs-oleate precursor (dissolving 0.4g $CsCO_3$ in 16.5 ml OA) was swiftly injected. After injection, the sample was cooled down immediately using ice bath.

The $CsPbI_3$ nanowires were synthesized with the following procedure: 5 mL ODE, 0.0168g PbI2, 250 μL oleic acid, 250 μL oleylamine, 500 μL octylamine and 500 μL octanoic acid were loaded into a 25 mL 3-neck flask and dried under vacuum for 20 minutes at 100 °C. After complete solubilization of the PbI_2 salt, the temperature was increased to 160 °C under N_2 and 1 mL of Cs-oleate solution (this was prepared as follows: 0.032 g Cs_2CO_3 and 10 mL oleic acid were loaded into 25 mL 3-neck flask, dried for 1h at 120 °C under vacuum, and then heated under N_2 to 140 °C until all Cs_2CO_3 reacted with oleic acid) was swiftly injected. After 5 minutes, the reaction mixture was slowly cooled to room temperature using a water bath.

References

1. Egerton, R. F.; Li, P.; Malac, M. Radiation Damage in the Tem and Sem. *Micron* **2004**, *35*, 399-409.
2. Seah, M. P.; Dench, W. A. Quantitative Electron Spectroscopy of Surfaces: A Standard Data Base for Electron Inelastic Mean Free Paths in Solids. *Surf. Interface Anal.* **1979**, *1*, 2-11.